Pattern generation with synthetic sensing systems in lipid bilayer membranes

Takeuchi, Toshihide; Montenegro, Javier; Hennig, Andréas; Matile, Stefan

How to cite

TAKEUCHI, Toshihide et al. Pattern generation with synthetic sensing systems in lipid bilayer membranes. In: Chemical science, 2011, vol. 2, n° 2, p. 303–307. doi: 10.1039/c0sc00386g

This publication URL: https://archive-ouverte.unige.ch/unige:13220
Publication DOI: 10.1039/c0sc00386g

Pattern Generation with Synthetic Sensing Systems in Lipid Bilayer Membranes

Toshihide Takeuchi,[a,b,c] Javier Montenegro,[a,b] Andreas Hennig,[a,d] and Stefan Matile*[a]

The objective of this study was to introduce differential sensing techniques to synthetic systems that act, like olfactory receptors, as transporters in lipid bilayer membranes. Routine with most alternative chemosensing ensembles, pattern generation has, quite ironically, remained inaccessible in lipid bilayers because the number of available crossresponsive sensor components has been insufficient. To address this challenge, we here report on the use of cationic hydrazides that can react in situ with hydrophobic analytes to produce cationic amphiphiles which in turn can act as countercation activators for polyanionic transporters in fluorogenic vesicles. To expand the dimension of signals generated by this system, a small collection of small peptides containing a positive charge (guanidinium, ammonium) and one to three reactive hydrazides are prepared. Odorants are used as examples for hydrophobic analytes, perfumes to probe compatibility with complex matrices, and counterion-activated calf-thymus DNA as representative polyion-counterion transport system. Principal component and hierarchical cluster analysis of the obtained multidimensional patterns are shown to differentiate at least 21 analytes in a single score plot, discriminating also closely related structures such as enantiomers, *cis-trans* isomers, single-atom homologs, as well as all tested perfumes. Inverse detection provides access to analytes as small as acetone. The general nature of the introduced methodology promises to find diverse applications in current topics in biomembrane research.

Introduction

In mammalian olfactory systems, about 350 olfactory receptors recognize more than 10'000 different odorants.[1] Incompatible with 1:1 recognition by individual receptors, these biological sensing systems use less specific interactions with several receptors to generate patterns that are recognized as unique "fingerprints" by the brain. Attractive because little discriminatory power is needed for signal generation, these lessons from nature have been successfully applied to several chemosensor systems.[2-17] The bottleneck of this approach is the establishment of multiple molecular recognition frameworks, which are necessary to generate patterns. So far, this has not been possible with synthetic sensing systems that work, like olfactory receptors, in lipid bilayer membranes.[18-31] The objective of this study was to change this situation, using odorants **O1-O30** as illustrative collection of challenging analytes with high similarity (Fig. 1).

Hydrophobic analytes in general are problematic with established membrane-based synthetic sensing systems because they tend to simply disappear in the hydrophobic membrane instead of interacting with synthetic pores[26-28] or activating polyion transporters.[29-31] This problem has been solved with the *in-situ* introduction of hydrophilic headgroups that can react with hydrophobic analytes to afford amphiphilic counterions which, in turn, can activate polyion transporters and generate a "turn-on" fluorescent response (Fig. 1).[29] The transport processes involved in this sensing scheme have been studied in detail for both polyanion[30,31] and polycation transporters.[29] To introduce differential sensing approaches[2-10] to synthetic systems that operate in lipid bilayers,[18-31] it occurred to us that a collection of different reactive counterions could already be sufficient to generate analyte-specific fingerprints. As reported in the following, this turned out to be true.

Results and Discussion

Reactive counterions **A1H1-A1H3** and **G1H1-G1H3** were designed and synthesized to explore differential sensing in lipid bilayer membranes (Fig. 1). They all contain either an ammonium (**A1H1-A1H3**) or a guanidinium cation (**G1H1-G1H3**) to interact with polyanionic DNA transporters, and one to three hydrazides to capture odorants by hydrazone formation.[27,29,32-34] Details on their synthesis can be found in the Supporting Information (Figs. S1-S3).[35] Incubation of 30 fragrant aldehydes and ketones **O1-O30** with the six hydrazides **A1H1-A1H3** and **G1H1-G1H3** gave rapid access to 180 cationic amphiphiles **A1H1O1-G1H3O30** with little synthetic effort. Their ability to activate polyanion transporters was explored under routine conditions, using calf-thymus (ct) DNA as polyanion transporter acting in EYPC-LUVs⊃HPTS/DPX (*i.e.*, egg yolk phosphatidylcholine large unilamellar vesicles loaded with the anionic fluorophore 8-hydroxy-1,3,6-pyrenetrisulfonate and the cationic quencher *p*-xylene-bis-pyridinium bromide).[30,31] This assay reports transport activity as fluorescence recovery due to release of at

[a]*Department of Organic Chemistry, University of Geneva, Geneva, Switzerland. Fax: +41 22 379 5123; Tel: +41 22 379 6523; E-mail: stefan.matile@unige.ch; www.unige.ch/sciences/chiorg/matile/*

[b]*These two authors contributed equally to this work.*

[c]*Current address: Department of Degenerative Neurological Diseases, National Institute of Neuroscience, National Center of Neurology and Psychiatry, Tokyo, Japan*

[d]*Current address: BAM Federal Institute for Materials Research and Testing, Bioanalytical Chemistry and Fluorescence Spectroscopy, Berlin, Germany*

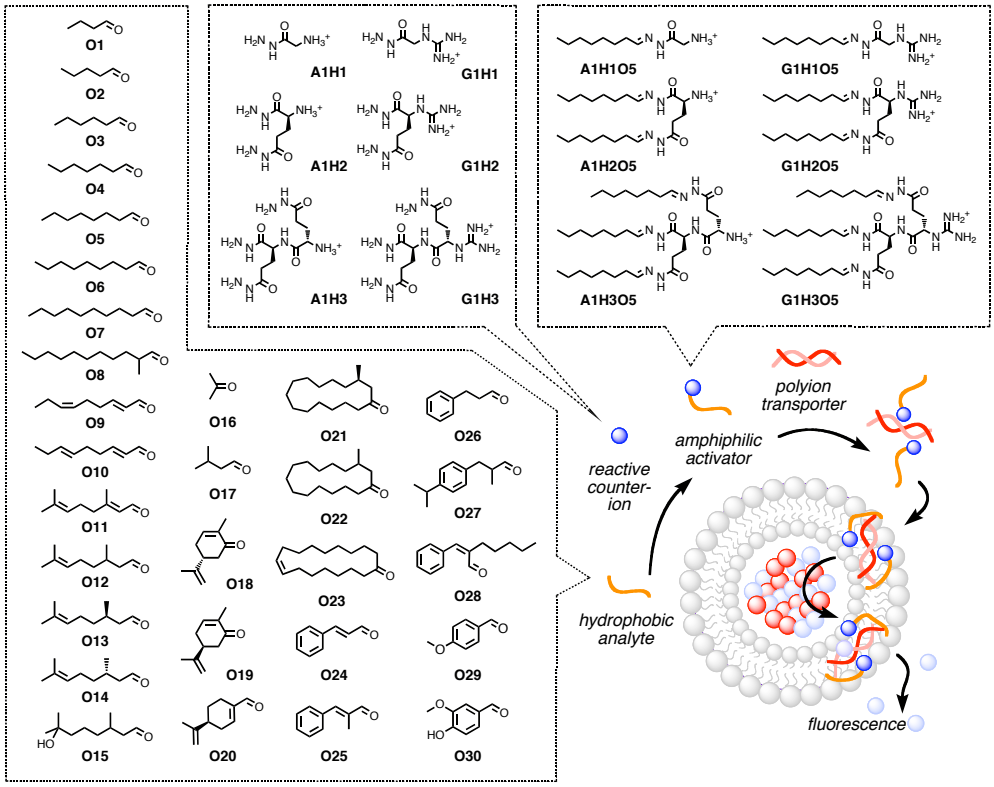

Fig. 1. Sensing scheme for fragrance sensing by pattern generation in fluorogenic vesicles. Hydrophobic analytes (*e.g.*, odorants **O1-O30**) are incubated with hydrophilic reactive counterions (*e.g.*, **A1H1-A1H3**, **G1H1-G1H3**) to give amphiphilic counterions (*e.g.*, **A1H1O5-A1H3O5**, **G1H1O5-G1H3O5**) that activate polyions (*e.g.*, ctDNA) in lipid bilayer membranes (*e.g.*, fluorogenic vesicles). Citral **O11** is a mixture of *cis*- (neral) and *trans*-isomers (geranial).

least the quencher DPX[31] from the vesicles (Fig. S4A). Characteristic parameters are EC_{50}, the effective concentration needed to reach 50% of Y_{MAX}, the maximal accessible activity, and n, the Hill coefficient, which can all be obtained from Hill analysis of single dose response curves (Figs. S4B, 2A, etc).

Pattern generation was exemplified first for octanal **O5**, a citrus odorant used for flavor production in food industry. The dose response curves for **A1H1O5-A1H3O5** and **G1H1O5-G1H3O5** revealed an increasing ability to activate DNA transporters with increasing number of tails and decreasing acidity of the cation (Fig. 2A, for other odorants, see Fig. S5). For pattern generation, dose response curves were recorded for increasing concentrations of odorant **O5** after incubation with **A1H2**, **A1H3**, **G1H2** and **G1H3** at constant concentrations (Fig. S6). The three independent readouts EC_{50}, Y_{MAX} and n obtained for four counterion activators yielded a 12-dimensional pattern for **O5** (Fig. 2B, row 1). Application of the same routine to **O11, O12**, **O20**, **O24** and **O26** gave a collection of 12D fingerprints for 6 analytes (Fig. 2B). Among odorants **O3-O30**, this method of pattern generation worked under identical conditions. However, odorants **O3, O18**, **O19** and **O21-O23** are shown as examples where slightly higher hydrazide concentrations produce nicer patterns, and **O15-O17**, **O29** and **O30** as examples that give best patterns by inverse detection (Fig. S7, see below). Three independent experiments were performed per analyte to determine reproducibility and experimental error; the result was excellent (Figs. 2D, 3A, 3C; Tables S2, S3).

The obtained patterns were subjected to hierarchical clustering (HCA) and principal component analysis (PCA).[2] HCA is an unsupervised method of multivariant analysis that converts interpoint Euclidean distances between all samples in the n-dimensional space into 2D dendrograms (Fig. 2C). PCA concentrates the most significant characteristics (variance) of the multidimensional pattern into lower dimensional space by calculating eigenvectors (principal components, PC) in the direction of maximal variances. This reduces the n-dimensional pattern to a single score that is then plotted in the new PC space (Fig. 2D). Both 2D HCA dendrogram and 3D PCA score plot obtained for 23 odorants demonstrated overlap-free discrimination. The HCA dendrogram showed clustering of some of the aromatic odorants (**O24-O26**, cluster 4) around 20 Euclidian distance units (E.u.). Other clusters found around 20 E.u. contained odorants with mostly unsaturated (**O9-O14**, cluster 3), saturated (**O5-O7**, etc, cluster 2) and cyclic alkyl tails (**O23** and perillaldehyde **O20**, main odorant of perilla leaves (or *Shiso* in Sashimi dishes)). Consistent with the structural similarities, the latter two clusters 1 and 2 merged around 30 E.u., whereas discrimination from unsaturated (cluster 3) and aromatic odorants (cluster 4) occurred around 45 E.u. and 120 E.u.,

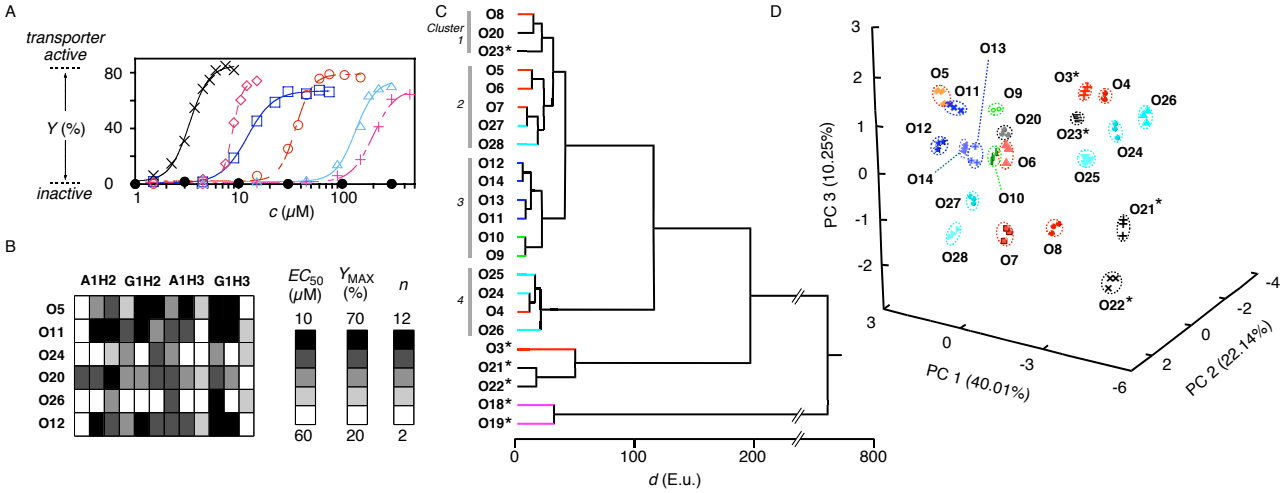

Fig. 2. Pattern generation and pattern recognition with cationic hydrazide activators and DNA transporters. (A) Dose response curves for the activation of ctDNA (1.25 μg/ml) in EYPC-LUVs⊃HPTS/DPX with amphiphiles **A1H1O5** (+), **G1H1O5** (△), **A1H2O5** (○), **G1H2O5** (◊), **A1H3O5** (□), **G1H3O5** (×) and **O5** (●), (B) 12D pattern generated for 6 odorants with 4 reactive counterions (**A1H2**, **G1H2**, **A1H3** and **G1H3**) and three readouts each (from left to right: Effective odorant concentration EC_{50}, the concentration needed to reach $Y_{MAX}/2$, maximal activity Y_{MAX}, Hill coefficient n). All data were obtained from Hill analysis of dose response curves for odorants **O** (variable concentration) coupled with reactive counterions (constant concentration, 50 μM (**A1H2**), 15 μM **G1H2**), 30 μM (**A1H3**) and 5 μM (**G1H3**) final concentration) and detected with ctDNA in HPTS/DPX-LUVs (constant concentrations, analog to (A)). (C) HCA dendrogram for 23 odorants, showing the Euclidian distances d between average values from three trials. (D) PCA score plot for 21 odorants (data points are from three independent experiments per analyte, made to determine reproducibility and experimental error, see Table S2). *Measured with 50 μM (**A1H2**), 30 μM (**G1H2**), 50 μM (**A1H3**) and 30 μM (**G1H3**, final concentrations), off-scale carvones **O18**/**O19** are omitted in (D), see ref 35 for details.

respectively. Several exceptions from these trends concerned either mixed motifs, present in the cyclamen aldehyde cyclosal **O27** and jasminaldehyde **O28**, or odorants with borderline activity such as the shortish heptanal **O4** (lost among aromatics) or the longish 2-methylundecanal **O8** (within cyclic odorants). Other odorants with weak activity such as hexanal **O3**, muscone **O21**/**O22** and carvone **O18**/**O19** (but not civetone **O23**) clustered far apart from the rest.

Overlap-free recognition of 23 odorants in HCA and PCA was highly remarkable for a solution-based supramolecular sensor array considering the similarity of the involved structures. The result demonstrated that nearly all challenges in supramolecular recognition (enantiodifferentiation, *cis*-*trans* isomerization, single-atom homologues, etc.) have been successfully addressed with a single, simple and straightforward to optimize system. For example, discrimination of close derivatives of cinnamaldehyde **O24** including 2-methylcinnamaldehyde **O25** or hydrocinnamaldehyde **O26** was no problem (Fig. 2D, top right; focused PCA, Fig. S9C). Discrimination of homologous linear alkyl aldehydes, from hexanal **O3** over heptanal **O4**, octanal **O5**, nonanal **O6** and decanal **O7** up to 2-methylundecanal **O8** occurred with unproblematic single-carbon resolution (global, Fig. 2D; focused, Fig. S9B).

Detectability of *cis*-*trans* stereoisomers was explored with 2*E*,6*Z*-nonadienal **O9**, the cucumber aldehyde with the diffusely "green" odor, and its 2*E*,6*E*-isomer **O10**. Their hydrazones obtained with **A1H2**, **A1H3**, **G1H2** and **G1H3** resembled *cis*- and *trans*-isomers of unsaturated phospholipids. Considering how the small structural difference between the latter has a big impact in lipid bilayer structure and function, we presumed that these isomers could be easily discriminated. In fact, HCA dendrogram and PCA score plots revealed overlap-free differentiation between the *cis*-isomer **O9**, the *trans*-isomer **O10** as well as the parent nonanal **O6** (Figs. 2C, 2D, 3C).

Enantiodiscrimination, a hallmark of the mammalian olfactory system, was explored first with (*R*)-(+)-citronellal **O13**, an antifungal insect repellant that accounts for the lemon scent of citronella oil. HCA dendrograms revealed full discrimination between (*R*)-(+)-citronellal **O13**, the (*S*)-(-)-enantiomer **O14**, their racemic mixture (±)-citronellal **O12** and nearly identical citral **O11** (Fig. 2C). Note that apparent close proximities in the global score plot (Fig. 2D, center left) are optical illusions due to graphical limitations as confirmed by focused PCA score plots (Fig. 3C).

Attached to **A1H2**, **A1H3**, **G1H2** and **G1H3,** the 15-membered ring of (*R*)-(-)-muscone **O21**, the legendary primary contributor to the odor of musk,[36] looked like two alkyl tails of a phospholipid that are linked together at the end. In the muscone hydrazone **G1H3O21**, this adds up to an amphiphile with six tails and a single charged head, creating *in situ* a complexity comparable to lipids such as cardiolipin. However, macrocyclic alkyl tails gave weaker response than linear alkyl tails. Slightly varied initial hydrazide concentrations were thus used for pattern generation. In the resulting PCA score plot, enantioenriched (*R*)-(-)-muscone **O21** (61% *ee*) was clearly separated from racemic (±)-

muscone **O22** (global, Fig. 2; focused, Fig. S9E). Differentiation from the structurally related civetone **O23**, a pheromone of the African civet composed of 17-membered cyclic ketone with a *cis*-alkene in position 8, was no problem (Figs. 2D, S9E). General validity of enantiodiscrimination with our supramolecular sensing system was corroborated with carvone. *R*-(-)-carvone **O18** smells like caraway, *S*-(+)-carvone **O19** smells like spearmint. Measured at slightly higher activator concentrations like muscone because of weak responsiveness, both enantiomers appeared cleanly separated in HCA dendrograms (Fig. 2C) and PCA score plots (Fig. S9E).

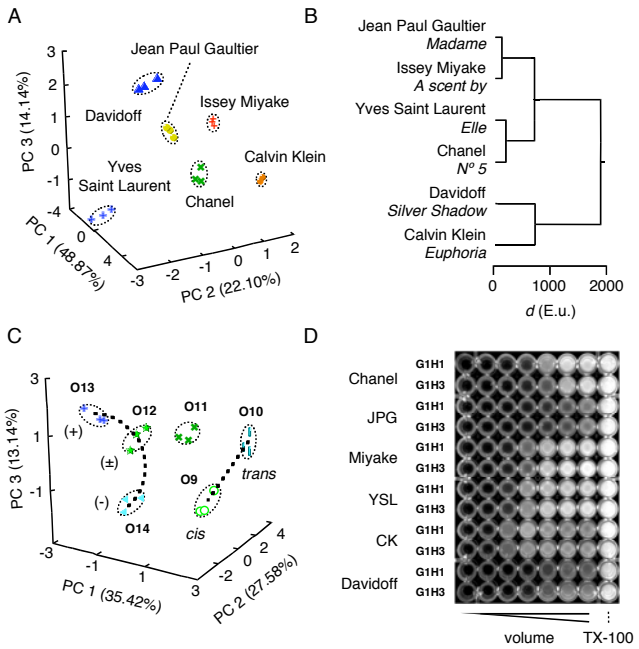

Fig. 3. Compatibility with complex matrices, enantiodiscrimination, discrimination of *cis-trans* isomers and high-throughput formats. (A) PCA score plot and (B) HCA dendrogram for arbitrarily selected perfumes. See Fig. 2 and ref. 35 for details. (C) Focused PCA score plot to corroborate detectability of enantiomers (**O12-O14**) and *cis-trans* isomers (**O9-O10**, dotted lines; from global PCA in Fig. 2D). Data points in (A) and (C) are from three independent experiments per analyte, determining experimental error, see Tables S2, S3). (D) Fluorescent image of multiwell plate. See ref. 35 for experimental details.

Compatibility of our new sensing system with samples from daily life was explored with randomly selected perfumes. A 12D pattern was generated as above, with **A1H2**, **A1H3**, **G1H2** and **G1H3** for analyte capture and DNA activation in DPX-vesicles (Fig. S8). PCA afforded a score plot where Chanel Nº 5, Jean Paul Gaultier's Madame, a scent by Issey Miyake, Elle from Yves Saint Laurent, Calvin Klein's Euphoria, and Silver Shadow from Davidoff are separated without overlap (Fig. 3A). In the HCA dendrogram, close similarity was found for Chanel Nº 5 and Elle around 100 E.u., whereas Euphoria and Silver Shadow (700 E.u.) were most distinct from the rest (1900 E.u., Fig. 3B).

To sense an analyte as small as acetone **O16**, direct detection failed because amphiphiles **A1H2O16**, **A1H3O16**, **G1H2O16** and **G1H3O16** were not hydrophobic enough to activate DNA transporters. Therefore, an inverse detection scheme was devised, wherein hydrazides **A1H2**, **A1H3**, **G1H2** and **G1H3** were incubated with constant concentration of active octanal **O5** and increasing concentration of inactive acetone **O16** serving as a competitor. Decreasing concentrations of **A1H2O5**, **A1H3O5**, **G1H2O5** and **G1H3O5** in the presence of increasing concentrations of acetone **O16** were then monitored as a decreasing fluorescence emission (Fig. S7). The same was also true for isovaleraldehyde **O17**, and the more hydrophilic hydroxycitronellal **O15**, anisaldehyde **O29** and vanillin **O30**. HCA dendrograms and PCA score plots obtained by inverse detection cleanly separated all tested analytes (Fig. S10).

Compatibility with multiwell assays was explored as hint toward potential for practice (Fig. 3D). HCA and PCA revealed that perfume recognition is possible also from the simplified patterns generated by less refined "high-throughput" methods under adjusted, clearly different conditions.

Conclusions

Whereas many wonderful, much more practical differential chemosensors have been reported over the past two decades,[2-10] this is the first synthetic differential sensing system that operates, like olfactory receptors, in lipid bilayer membranes. Experimental evidence is delivered for generation and recognition of composite responses or "fingerprints" at highest possible resolution (Fig. S11). This includes the simultaneous differentiation of 28 closely related odorants, covering enantiomers, *cis-trans* isomers, single-atom homologues, and so on. As an example for compatibility with complex matrices, we show that, like a human nose, perfumes can be smelled with neither knowing nor identifying their molecular composition.

The key conceptual advance of the introduced approach is that subtle structural differences are magnified covalently in dynamic oligomers as well as non-covalently on polyions and in lipid bilayers. Quite similar amplification of subtle structural differences is known from the distinct impact of enantiomers, *cis-trans* isomers and single-atom homologues of biological phospholipids and steroids on structure and function of biomembranes. For enantiodiscrimination, this effect is exploited in a highly "chiral" environment, including the use of chiral reactive couterions **A1H2**, **A1H3**, **G1H2** and **G1H3** to produce diastereomeric counterion activators for chiral polyion transporters in chiral lipid bilayer membranes.

The introduced approach excels with facile accessibility, exceptional modularity and broad applicability. This will allow to explore variations with regard to counterion activators (numbers of heads and tails, nature and position of charges, including charge inversions to add cell-penetrating peptides as transporters,[29,37] covalent capture chemistry (boronates,[11,28] enzyme-/aptamer-coupled capture,[26-29] etc[32-34]), polyion and membrane composition (including polymersomes[38]), readouts (including color,[39] circular dichroism, current, multiwell assays (Fig. 3D), chips, etc) and other applications (fragrant cellular uptake,[29,37,40] controlled release,[34] etc).

Acknowledgement

We thank J. Praz for contributions to synthesis, D. Jeannerat, A. Pinto and S. Grass for NMR measurements, the Sciences Mass Spectrometry (SMS) platform at the Faculty of Sciences, University of Geneva, for mass spectrometry services, H. Riezman and M. Umebayashi for access to the fluorescence imaging system, L. Wunsche and A. Herrmann (Firmenich, Geneva) for odorant samples, and the University of Geneva and the Swiss NSF for financial support.

to the fs-laser pulse.

References

1 L. B. Buck, *Angew. Chem. Int. Ed.*, 2005, **44**, 6128-6140.
2 J. C. Jurs, G. A. Bakken and H. E. McClelland, *Chem. Rev.*, 2000, **100**, 2649-2678.
3 J. J. Lavigne and E. V. Anslyn, *Angew. Chem. Int. Ed.*, 2001, **40**, 3118-3130.
4 S. H. Shabbir, L. A. Joyce, G. M. da Cruz, V. M. Lynch, E. Sorey and E. V. Anslyn, *J. Am. Chem. Soc.*, 2009, **131**, 13125-13131.
5 M. A. Palacios, R. Nishiyabu, M. Marquez and P. Anzenbacher Jr, *J. Am. Chem. Soc.*, 2007, **129**, 7538-7544.
6 B. A. Suslick, L. Feng and K. S. Suslick, *Anal. Chem.*, 2010, **82**, 2067-2073.
7 A. Buryak and K. Severin, *Angew. Chem. Int. Ed.*, 2005, **44**, 7935-7938.
8 H. Zhou, L. Baldini, J. Hong, A. J. Wilson and A. D. Hamilton, *J. Am. Chem. Soc.*, 2006, **128**, 2421-2425.
9 D. C. Gonazlez, E. N. Savariar and S. Thayumanavan, *J. Am. Chem. Soc.*, 2009, **131**, 7708-7716.
10 N. T. Greene and K. D. Shimizu *J. Am. Chem. Soc.*, 2005, **127**, 5695-5700.
11 G. Mirri, S. D. Bull, P. N. Horton, T. D. James, L. Male and J. H. Tucker, *J. Am. Chem. Soc.*, 2010, **132**, 8903-8905.
12 A. Satrijo and T. M. Swager, *J. Am. Chem. Soc.*, 2007, **129**, 16020-16028.
13 C. Guarise, L. Pasquato, V. De Filippis and P. Scrimin, *Proc. Natl. Acad. Sci.*, 2006, **103**, 3978-3982.
14 A. Wada, S. Tamaru M. Ikeda and I. Hamachi, *J. Am. Chem. Soc.*, 2009, **131**, 5321-5330.
15 M. Florea and W. M. Nau, *Org. Biomol. Chem.*, 2010, **8**, 1033-1039.
16 J.-L. Reymond, V. S. Fluxa and N. Maillard, *Chem. Commun.*, 2009, **45**, 34-46.
17 L. Vial and P. Dumy, *New J. Chem.*, 2009, **33**, 939-946.
18 A. P. Davis, D. N. Sheppard and B. D. Smith, *Chem. Soc. Rev.*, 2007, **36**, 348-357.
19 C. P. Wilson and S. J. Webb, *Chem. Commun.*, 2008, **44**, 4007-4009.
20 A. Satake, M. Yamamura, M. Oda and Y. Kobuke, *J. Am. Chem. Soc.*, 2008, **130**, 6314-6315.
21 X. Li, B. Shen, X. Q. Yao and D. Yang, *J. Am. Chem. Soc.*, 2009, **131**, 13676-13680.
22 G. W. Gokel and N. Barkey, *New J. Chem.*, 2009, **33**, 947-963.
23 J. T. Davis, P. A. Gale, O. A. Okunola, P. Prados, J. C. Iglesias-Sanchez, T. Torroba and R. Quesada, *Nat. Chem.*, 2009, **1**, 138-144.
24 R. E. Dawson, A. Hennig, D. P. Weimann, D. Emery, S. Gabutti, J. Montenegro, V. Ravikumar, M. Mayor, J. Mareda, C. A. Schalley and S. Matile, *Nat. Chem.*, 2010, **2**, 533-538.
25 J. K. W. Chui and T. M. Fyles, *Chem. Commun.*, 2010, **46**, 4169-4171.
26 G. Das, P. Talukdar and S. Matile, *Science*, 2002, **298**, 1600-1602.
27 S. Litvinchuk, H. Tanaka, T. Miyatake, D. Pasini, T. Tanaka, G. Bollot, J. Mareda and S. Matile, *Nat. Mater.*, 2007, **6**, 576-580.
28 S. Hagihara, H. Tanaka and S. Matile, *J. Am. Chem. Soc.*, 2008, **130**, 5656-5657.
29 S. M. Butterfield, T. Miyatake and S. Matile, *Angew. Chem. Int. Ed.*, 2009, **48**, 325-328.
30 T. Takeuchi and S. Matile, *J. Am. Chem. Soc.*, 2009, **131**, 18048-18049.
31 T. Takeuchi, V. Bagnacani, F. Sansone and S. Matile, *ChemBioChem*, 2009, **10**, 2793-2799.
32 O. Ramström and J.-M. Lehn, *Nat. Rev. Drug Discov.*, 2002, **1**, 26-36.
33 P. T. Corbett, J. Leclaire, L. Vial, K. R. West, J. L. Wietor, J. K. M. Sanders and S. Otto, *Chem. Rev.*, 2006, **106**, 3652-3711.
34 A. Herrmann, *Org. Biomol. Chem.*, 2009, **7**, 3195-3204.
35 See Supporting Information.
36 L. Ruzicka, *Helv. Chim. Acta*, 1926, **9**, 715-729.
37 J. B. Rothbard, T. C. Jessop, R. S. Lewis, B. A. Murray and P. A. Wender, *J. Am. Chem. Soc.*, 2004, **124**, 9506-9507.
38 M. Kumar, M. Grzelakowski, J. Zilles, M. Clark and W. Meier, *Proc. Natl. Acad. Sci. USA*, 2007, **104**, 20719-20724.
39 S. M. Butterfield, A. Hennig and S. Matile, *Org. Biomol. Chem.*, 2009, **7**, 1784-1792.
40 S. Bhattacharya and A. Bajaj, *Chem. Commun.*, 2009, **45**, 4632-4656.

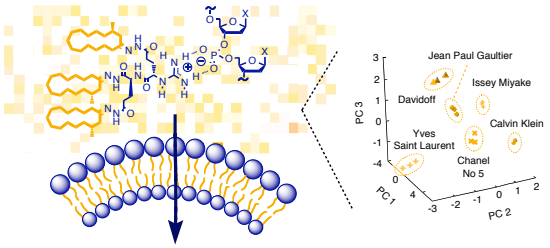

The first synthetic system that operates, like biological olfactory systems, by differential sensing in lipid bilayers is reported.